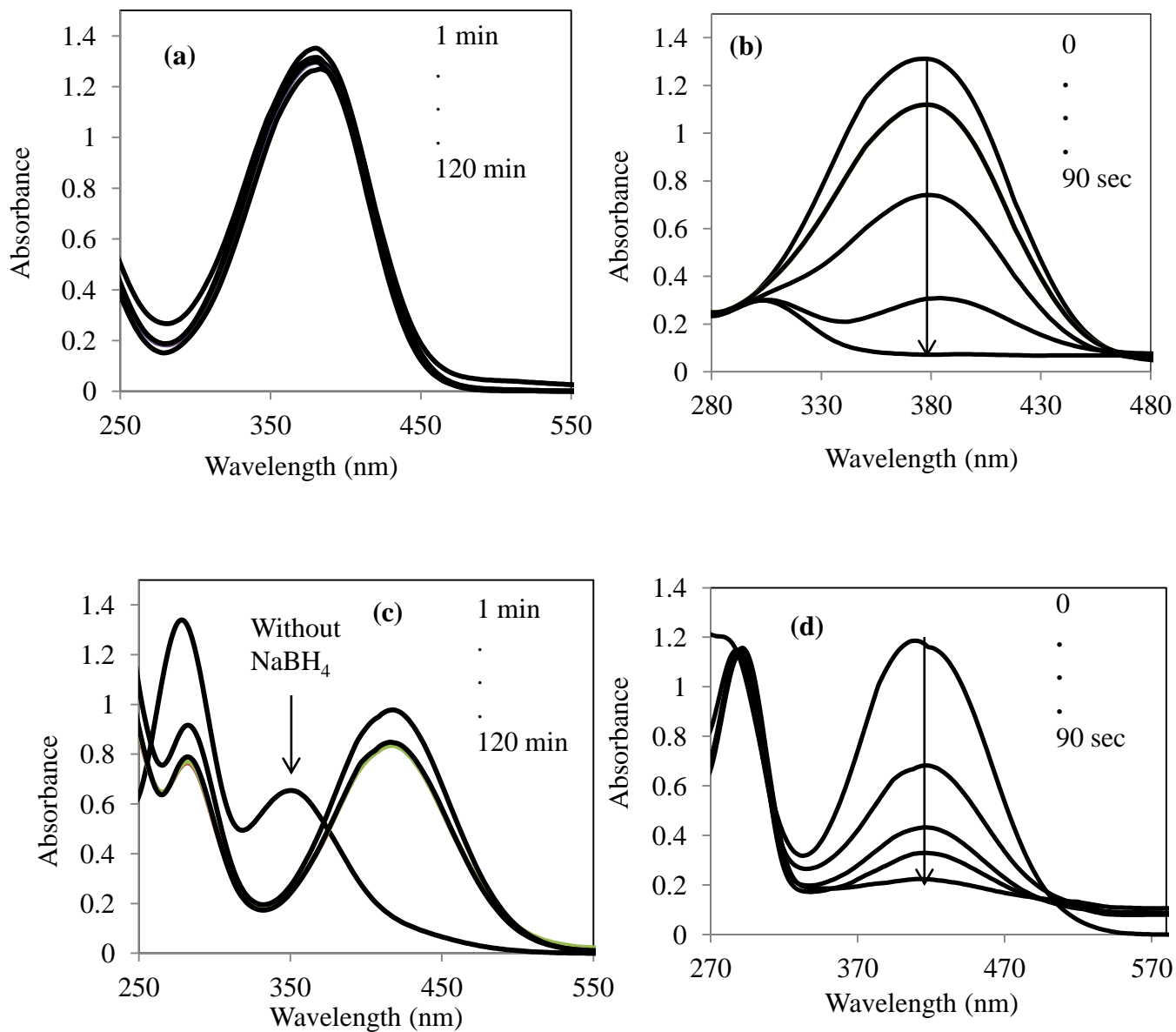
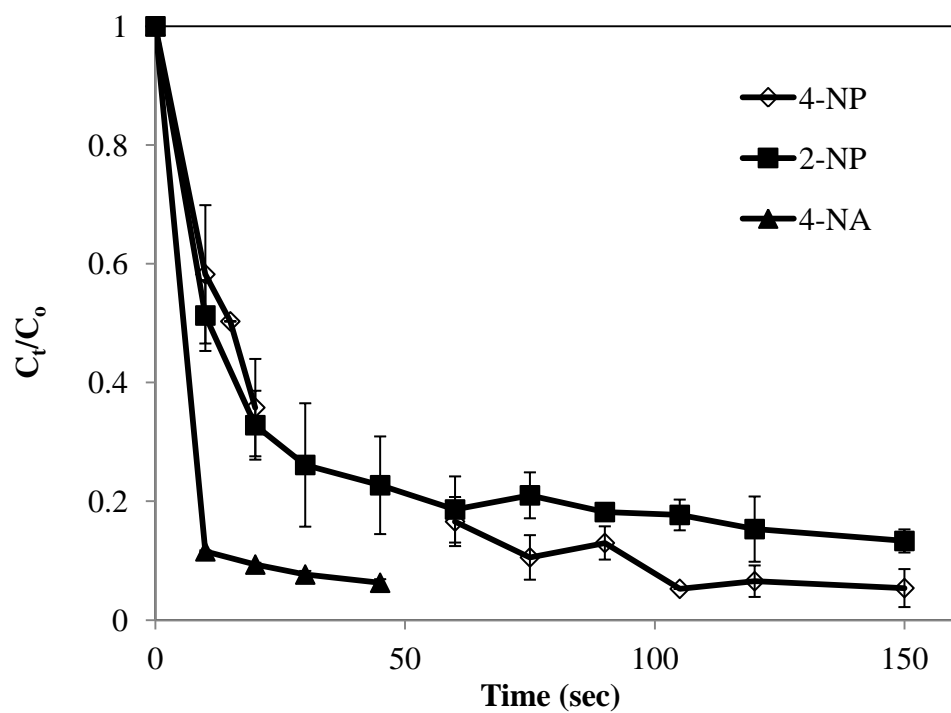


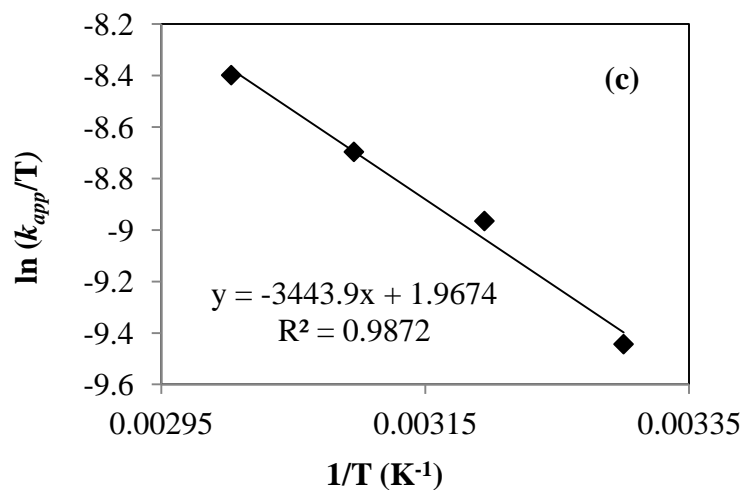
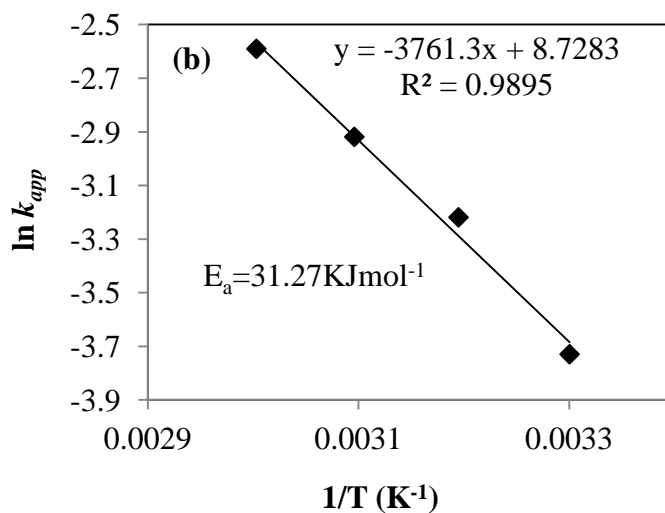
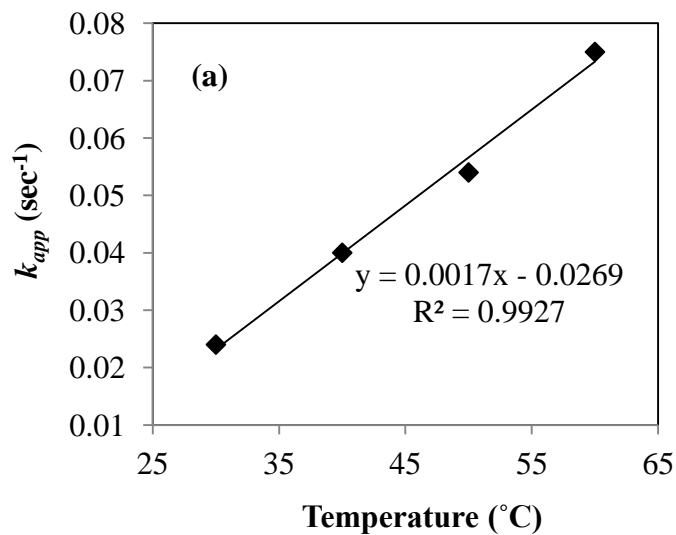
**Supporting Figure S1.** TEM Images of metal nanoparticles containing P(MAc) microgels (a) P(MAc)-Ni (b) P(MAc)-Cu and (c) P(MAc)-Co and (d) Thermograms of bare and composite microgels



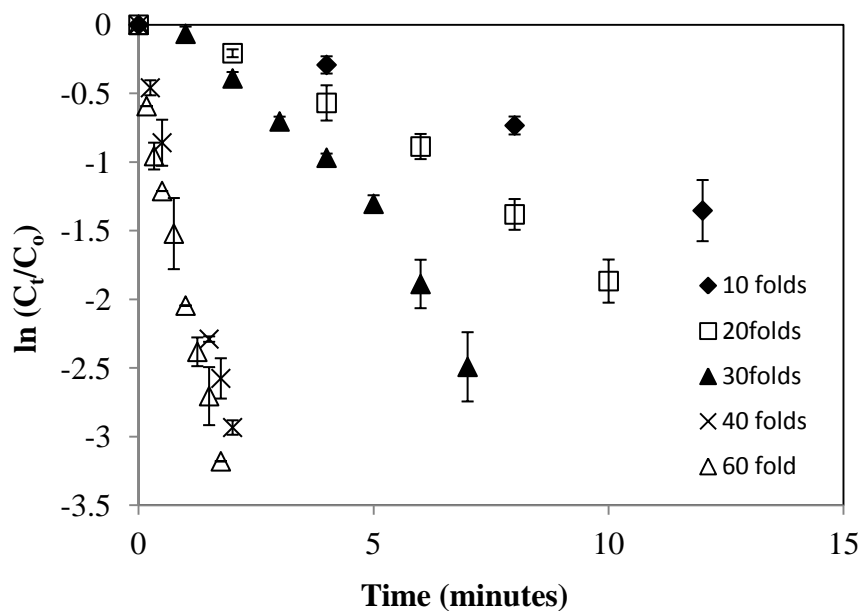
**Supporting Figure S2.** UV-Visible spectra of reduction of 2-NP (a) in the absence and (b) presence of p(MAc)-Cu composites, and for the reduction of 4-NA (c) in the absence (d) and presence of p(MAc)-Cu composites at 30°C.



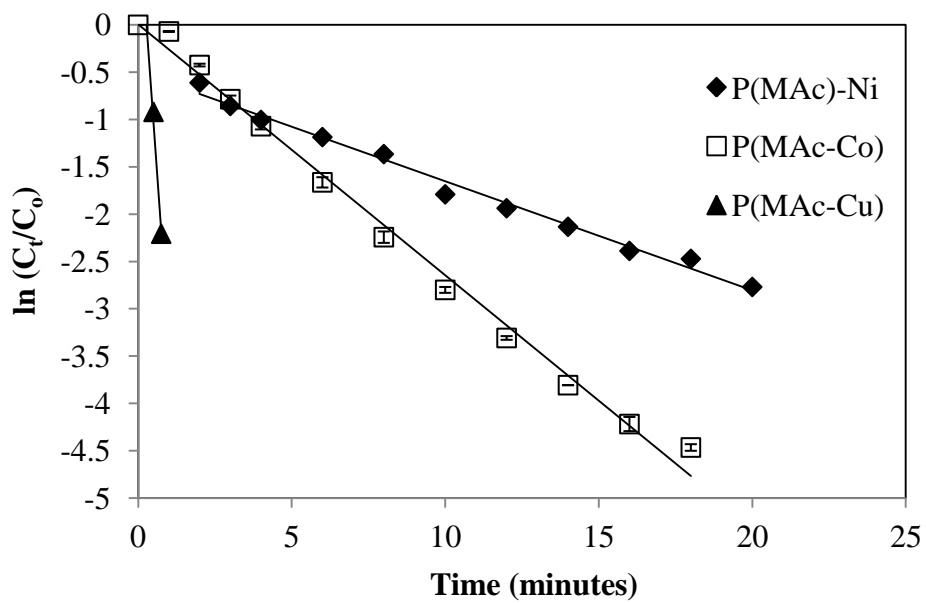
**Supporting Figure S3.** Catalytic performances of p(MAC)-Cu composites for the reduction of nitro aromatic compounds at 30°C under same reaction conditions.



**Supporting Figure S4.** (a) Plots of  $\ln(C_t/C_0)$  vs time for the reduction of 4-NP catalyzed by p(MAc)-Cu microgel composite at different temperatures, and (b) plot of  $\ln k_{app}$  vs  $1/T$ , and (c) plot of  $\ln(k_{app}/T)$  vs.  $1/T$ .



**Supporting Figure S5.** Change in values of  $k_{app}$  with the change in of amount of reducing agent during the reduction of 4-NP.



**Supporting Figure S6.** Plot of  $\ln(C_t/C_0)$  vs time for the catalytic degradation of Methyl Orange by p(MAc)-M (M: Cu, Co and Ni) microgel composite system.